

Chitosan Coating on Quartz Crystal Microbalance Gas Sensor for Isopropyl Alcohol and Acetone Detection

Nurul Liyana Lukman Hekiem¹, Aliza Aini Md Ralib^{1*}, MH Maziaty Akmal², Farah B. Ahmad³, Rosminazuin Ab Rahim¹, Nor Farahidah Za'bah¹ Gandhi Sugandi⁴

¹Department of Electrical and Computer Engineering,
International Islamic University Malaysia, Jalan Gombak, Kuala Lumpur, 53100, MALAYSIA

²Science Engineering Department,
International Islamic University Malaysia, Jalan Gombak, Kuala Lumpur, 53100, MALAYSIA

³Department of Biotechnology Engineering,
International Islamic University Malaysia, Jalan Gombak, Kuala Lumpur, 53100, MALAYSIA

⁴Research Center for Electronics and Telecommunications,
Indonesian Institute of Sciences, Jl Cicitu, Sangkuriang Bandung, Jawa Barat, INDONESIA

*Corresponding Author

DOI: <https://doi.org/10.30880/ijie.2022.13.03.026>

Received 14 January 2022; Accepted 07 June 2022; Available online 20 June 2022

Abstract: The development of acoustic wave sensors was driven by the presence of modern technology. Quartz crystal microbalance (QCM) has excellent sensing capabilities and has wide range of applications. Selection of sensing layer is crucial to ensure the performance of the QCM sensor for volatile organic compound (VOC) detection. Hence, the objective of this paper is to compare the performance of chitosan coated QCM sensor for different analyte gas: isopropyl alcohol (IPA). Finite element simulation was implemented using COMSOL Multiphysics to study the resonance frequency shift before and after sensing. Simulation results shows IPA detection shows a higher resonance frequency shift of 62.5 Hz compared to acetone due to higher molar mass. Experimental work is conducted to validate the simulation results where IPA analyte gas yields in 84.8 Hz which is higher than acetone analyte gas at 41.8 Hz. The functional groups for both sensing layer and analyte gas also affects the gas detection performance. IPA analyte gas possessed hydroxyl groups that favors to hydrogen bond formation with chitosan sensing layer. Thus, the QCM sensor with chitosan as the sensing layer has the potential for VOC sensing of different molar mass and functional groups.

Keywords: chitosan sensing layer, QCM sensor, resonance frequency shift, sensitivity

1. Introduction

Volatile organic compounds (VOCs) are organic substances that readily create vapours in ambient [1] and can be classified of alcohol, ketone, aldehyde, alkane, and aromatic compounds [2]. VOCs such as acetone [3], and isopropyl alcohol [4] are commonly known as biomarkers to detect cancerous diseases and may exert harmful effect when overexposed [5]. Aside from that, VOCs may also contribute to environmental pollution that causes global warming, for example having excess methane and carbon dioxide emitted from the vegetation of palm oil plantations [6][7].

Furthermore, excessive exposure to formaldehyde and alcohol in the air can cause chronic respiratory and cardiovascular problems, which can lead to mortality [8]. Gas sensing is extensively developed in diseases diagnosis, and environmental standards control [9]. Mass-sensitive sensor interprets the mass change detected into acquired measures. QCM is a type of mass-sensitive piezoelectric sensor which is a highly sensitive sensor that can provide rapid detection [10]. Acoustic wave propagated through the QCM from the voltage supplied to the QCM is converted back to electrical signal and measured in terms of resonance frequency as the output. The change in the resonance frequency is due to the mass change on the QCM sensor where wave damping occurs [11].

Sensing layer is crucial to investigate selectivity and sensitivity of the sensor towards analyte gases. Commonly used material as sensing layers are metal oxide [12], carbon nanotubes [13] and polymers [14]. Chitosan is a natural biopolymer composed of a polysaccharide chain formed by the deacetylation of chitin [15]. It's known for its mechanical strength, biodegradability, permeability, and film forming abilities [15]. It also has two reactive functional groups: the hydroxyl group and the amino group [15]. Because of these properties, chitosan can be modified in various ways to make it ideal for targeted gas detection. Experimental work was conducted using chitosan as a sensing layer on QCM sensor to detect VOCs; alcohols and aliphatic amines [16]. The authors also continued their studies on chitosan by modification with polyaniline PANI, a synthetic polymer [17]. Chitosan has been discovered to be a viable choice for a sensing layer since the results reveal that selectivity can be attained for aliphatic amines rather than alcohols [16], [17].

However, there are few investigations on acoustic wave sensor finite element simulations using chitosan sensing layers for QCM sensors. The objective of this paper is to analyze the performance of QCM sensor with chitosan sensing layers for IPA and acetone detection. The frequency shift performance of the QCM sensor using both sensing layers will be explored further throughout the study. This work presents the finite element simulation and experimental work for QCM sensor in detecting acetone and IPA analyte gases by using chitosan as the sensing layer.

2. COMSOL Multiphysics Simulation

2.1 Design Concept

The oscillation will be occurred at the quartz substrate when the alternating electric field applied over the top electrodes of the quartz crystal microbalance (QCM). Hence, the transverse acoustic wave propagates across the quartz substrate and being captured by the bottom electrode of the QCM. The resonance frequency of the QCM was designed to work at about 10 MHz in range. The resonance frequency is obtained following equation (1) where f is the resonance frequency, d is the thickness of the quartz substrate and v is the velocity of the acoustic wave.

$$f = \frac{v}{2d} \quad (1)$$

When the QCM is exposed to the analyte gas after sensing layer deposition, resonance frequency shift is observed due to the change in mass and velocity of the wave propagating through the quartz crystal substrates as shown in equation (2). The design parameter of QCM was designed as shown in Table 1 using 3D model. Fig.1(a) shows the geometry of the QCM sensor. The orientation of the AT-cut quartz follows the standards of IEEE standard of 1987 [18]. The structure of QCM substrate are thin gold electrodes of 200 nm thickness and 3 mm radius sandwiched between the quartz substrates. chitosan sensing layer was added on top of the gold electrode at 120 μm thickness. The model was given proper boundary conditions, and solid mechanics, electrostatics, and an electrical circuit were all incorporated into the relevant components. A mesh has been constructed and mapped onto the integrated and specified boundary condition model as shown in Fig. 1(b). Chitosan was chosen as the sensing layer for this work. Chitosan layer was deposited on top of the top gold electrode as shown in Fig. 1(d). The displacement of the wave propagating through the QCM sensor with and without chitosan sensing layer respectively was observed in Fig. 1(c) and Fig. 1 (d).

Table 1 - The design parameter set for COMSOL simulation on acetone and IPA analyte gas detection on QCM with chitosan sensing layer

Material	Description	Dimension
Quartz substrate	Radius	6.95 [mm]
	Thickness	167 [μm]
Gold Electrode	Radius	3 [mm]
	Thickness	200 [nm]
Chitosan sensing layer	Density	0.982 [g/cm^3]
	Young's Modulus	1.5 [GPa]
	Thickness	120 [μm]
Acetone	Molar mass	58.08 [g/mol]
IPA		60.1 [g/mol]

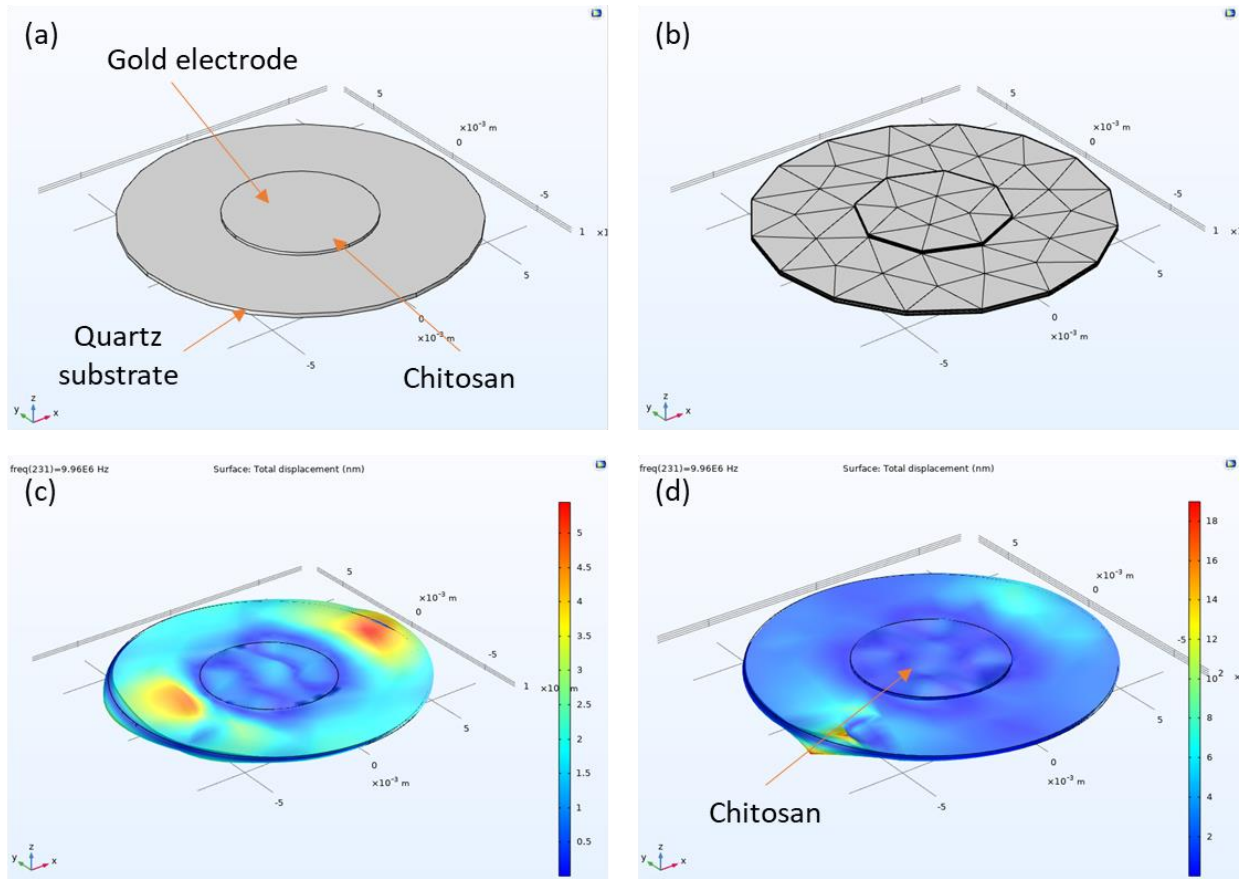


Fig. 1- (a) Structure of QCM sensor that consist of with top electrode, bottom electrodes and chitosan sensing layer; (b) Mesh structure for finite element FEM simulation; (c) Mode displacement of acoustic wave propagation without chitosan sensing layer; (d) Mode displacement of acoustic wave propagation with chitosan as sensing layer

The finite element simulation is then completed by applying the model to the allocated adaptive frequency sweep study, which yields the displacement curve. The resonance frequency for every change in the parameter was found from the displacement curve [19]. The sensitivity, S of the QCM sensor was calculated by finding the slope of frequency shift, Δf and mass change, Δm as shown in equation (2)[19].

$$S = \frac{\Delta f}{\Delta m} \quad (2)$$

2.2 Results and Discussion

2.2.1 Structure

The acoustic wave displacement of propagated across the sensor for QCM coated with chitosan is illustrated in Fig. 1 (d). The properties of the sensing layer deposited onto the QCM electrodes determined the wave propagation in terms of total displacement. These can be presented in the graph of frequency vs displacement as shown in Fig. 2. The resonance frequency of the QCM with gold electrode overlayed with chitosan sensing layer obtained is 9.9480585 MHz as shown in Fig. 2 (a).

The study of performance of the sensor in terms of resonance frequency shift and sensitivity were analysed by simulating the sensor response in two different VOCs gases: IPA and acetone at 1000 ppm concentration. The resonance frequency shifted to the left when there is change in mass on detected on the QCM sensor electrode and in agreement with Sauberry equation shown in (2). The exposure of the QCM sensor with chitosan sensing layer to the acetone and IPA analyte gases results in shifted resonance frequency to 9.947998 MHz and 9.947996 MHz as shown in Fig. 2 (b) and Fig. 2 (c). The sensing performance of the QCM sensor increases with increase in molar mass of the analyte gas. Hence,

the frequency shift obtained for IPA analyte gas is 62.5Hz greater than acetone analyte gas that is 60.5Hz. This is due that the molar mass for IPA (60.1 g/mol) is slightly higher than molar mass of acetone (58.08 g/mol) as shown in Table 1. Since the molar mass for acetone and IPA did not vary as much, small changes of resonance frequency shift (2 Hz) were observed. These results are in agreement with [20] where the changes in value of the resonance frequency indicates the addition of mass on the QCM sensor.

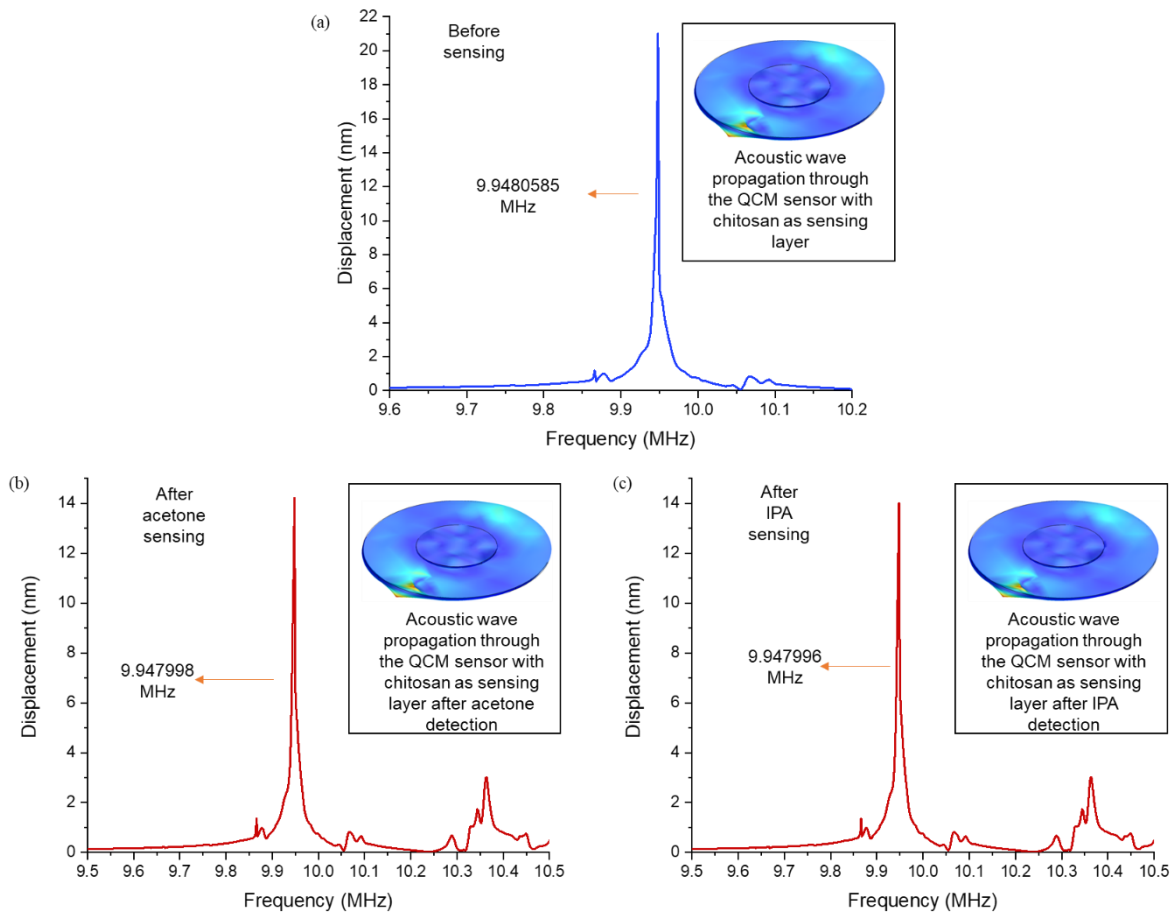


Fig. 2 - The graph of displacement against frequency obtained from finite element simulation where (a) resonance frequency of QCM before analyte gas sensing; (b) simulated resonance frequency when exposed to 1000 ppm acetone; (c) simulated resonance frequency when exposed to 1000 ppm IPA

Sensitivity is crucial to ensure the performance of the gas sensing. Sensitivity can be calculated from the slope of the graph resonance frequency shift against concentration of the analyte gas. The graph of resonance frequency shift against concentration of the analytes gases has been plotted as shown in Fig. 3. The slope value at 0.06076 Hz/ppm and 0.06232 Hz/ppm are the sensitivity value for chitosan sensing layer to acetone and IPA analyte gases respectively. A linear fit analysis gives R² values of 0.99993 and 0.99976 for acetone and IPA analyte gas detection consequently. The R² values indicates the precision of the data obtained to the theoretical estimation.

For both IPA and acetone detection using chitosan sensing layer, increase in concentration of analyte gas was observed when resonance frequency shift increases. Small change in molar mass of the two IPA and acetone gases has led to small variation to the detection as shown in Fig. 3. This agreed with the Sauerbrey's equation (3) where Δf is the resonance frequency shift, with f_o as the unperturbed frequency, Δm is the mass change, ρ as the density, A as the active area of the quartz substrate and μ as the shear modulus of quartz [21]. As the concentration of IPA and acetone increases, the resonance frequency shift also increases accordingly.

$$\Delta f = \frac{2f_o^2 \Delta m}{A\sqrt{\rho\mu}} \quad (3)$$

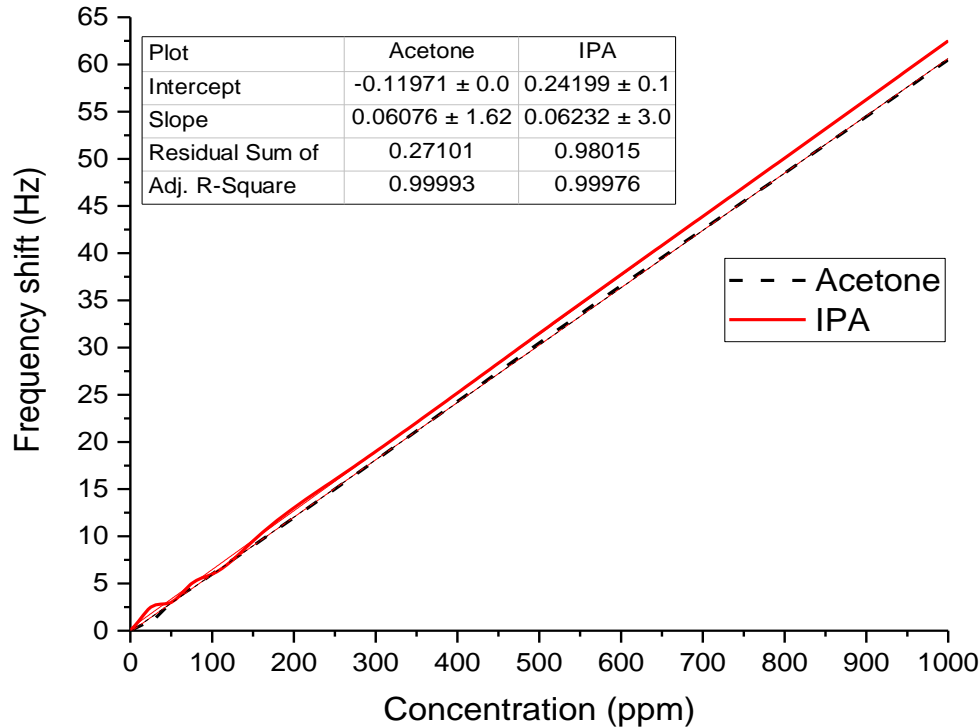


Fig. 3 - The sensitivity of the QCM sensor with chitosan sensing layer to acetone and IPA analyte gases which is obtained from the graph of resonance frequency shift against concentration of analyte gas

Chitosan as sensing layer is known as a natural biopolymer [22],[23]. It consists of hydroxyl group (-OH bond), carbonyl compounds, and aliphatic amines [20], [24], [25]. As for the analyte gases, acetone is in ketones group while IPA is an alcohol. Ketones are made up of carboxylic acids where it consists of carbonyl and carboxyl group (-COOH bond) [26] while alcohol consist of hydroxyl groups. These bonds are responsible for the adsorption of gas molecules. The detection of the IPA analyte gas is due to the formation of hydrogen bonds from the interaction of hydroxyl group in IPA analyte gas to the hydroxyl group in chitosan sensing layer [27]. Unfortunately, these interactions did not occur to alcohols. Acetone is highly polar, but it does not have any hydrogen atom attached to oxygen directly to enable any hydrogen bond formation [28]. Hence, only amines and carbonyl groups from chitosan sensing layer to interact with acetone [29]-[31]. These explains on the difference of resonance frequency shifts observed for both IPA and acetone gases.

3. Experimental Work

For validation purposes, an experimental work on acetone and IPA analyte gas detection has been implemented on 10 MHz QCM sensor with gold electrodes. Chitosan liquid solution was prepared by dissolving 0.5g of chitosan powder in 2% acetic acid solution with continuous stirring for 3 hours at 60°C. 5 µL of the prepared liquid solution was drop casted on the QCM electrode and dried in oven at 55°C for 30 minutes [20]. The QCM was then placed in a gas test chamber and connected to OpenQCM software as shown in Fig. 5. A micropipette was used to drop a volume of 5 µL analyte liquid into the gas test chamber and let to evaporate into gaseous state. The concentration ppm of the analyte gas in the gas test chamber was calculated using equation (4)[32] where ρ is the density of analyte liquid (g/mL), T is the gas test chamber (K), v is the analyte liquid volume (µL), M is the molecular weight of analyte gas (g/mol) and V is the volume of gas test chamber (L). The value of concentration in ppm calculated was 1720 ppm.

$$C = \frac{22.4\rho Tv \times 10^3}{273MV} \quad (4)$$

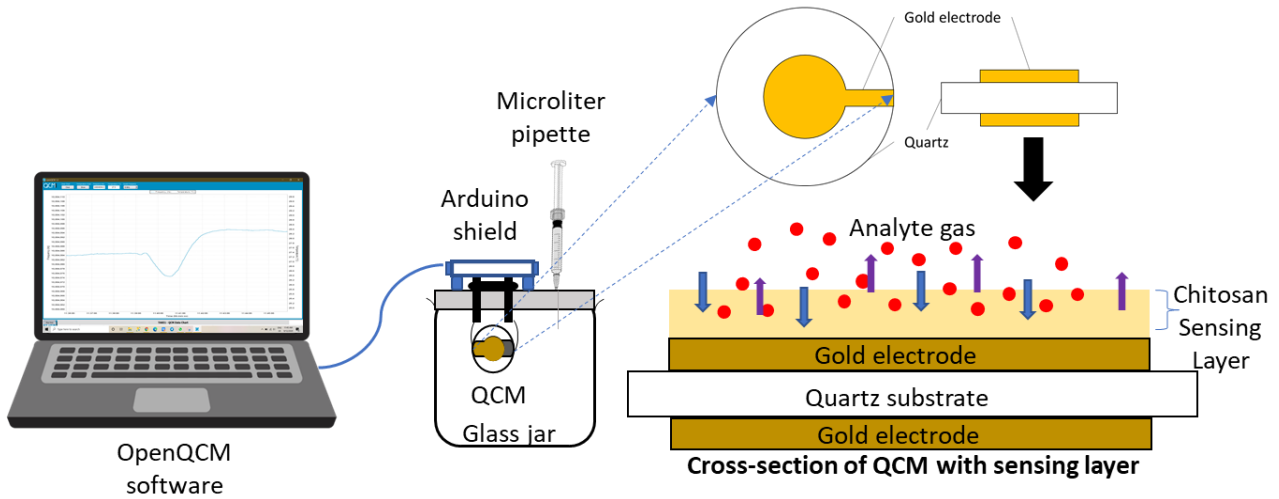


Fig. 4 - Experimental setup for acetone and IPA analyte gas sensing and the cross-section of the QCM sensor with the sensing mechanism.

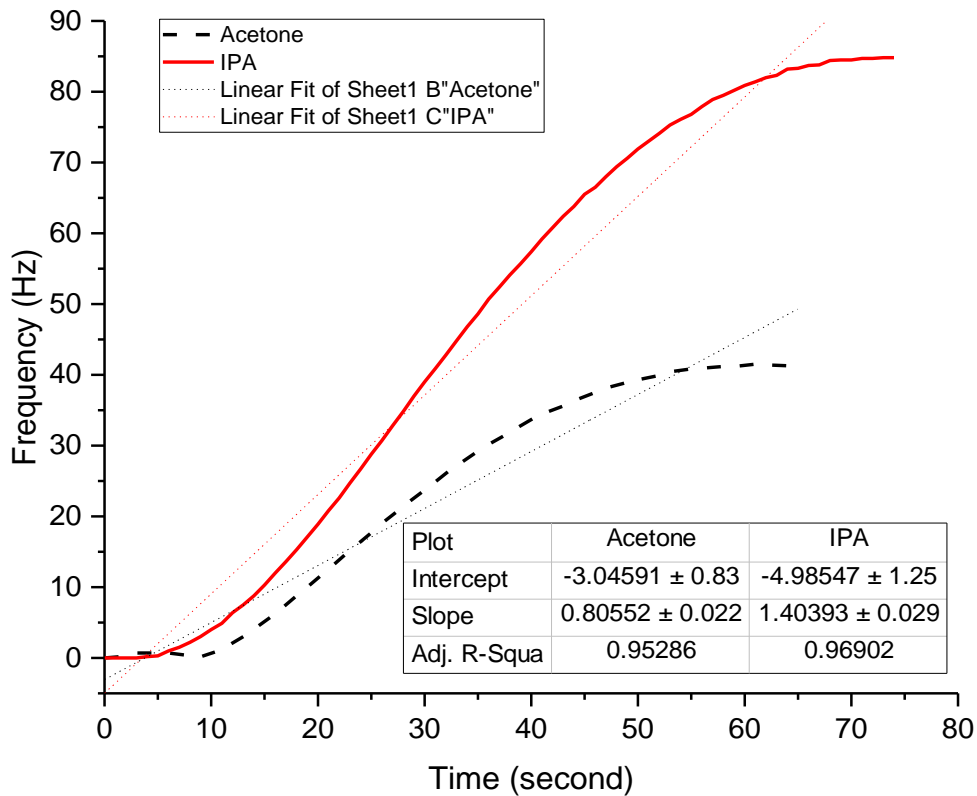


Fig. 5 - Graph of measured resonance frequency shift against time when QCM sensor with chitosan sensing layer is exposed to acetone and IPA analyte gases

The frequency measurements were recorded over time until it reached saturation where there is no further change was observed in frequency. Fig. 5 shows the graph of resonance frequency shift over time when QCM with chitosan sensing layer was exposed to both, acetone, and IPA analyte gases. From the graph, IPA analyte gas shows greater resonance frequency shifts at 84.8 Hz compared to acetone analyte gas at 41.3 Hz. The steepness of the slopes formed by linear fit analysis from the plots in Fig. 6 indicates the rate of adsorption in terms of resonance frequency shift by time. IPA analyte gas detection rate at 1.404 Hz/s is higher than acetone analyte gas which is at 0.806 Hz/s. This is due to the strong interaction between chitosan sensing layer and IPA analyte gas in the hydrogen bond formations [27].

The interaction between amines in chitosan sensing layer results in dehydrogenation of IPA analyte gas into carbonyl compounds also promotes to IPA analyte gas detection [33],[34]. The results of both simulation and experimental work have been summarized in Table 2.

Table 2 - Table of summary for simulated resonance frequency shift (Δf) for finite element simulation in comparison with measured resonance frequency shift (Δf) for experimental work

Analyte gas	Functional group	Molar mass (g/mol)	Finite element simulation Δf (Hz)	Experiment Δf (Hz)
Acetone	Ketone	58.08	62.5	84.8
IPA	Alcohol	60.1	60.5	41.3

4. Conclusion

In this work, chitosan layered on the electrode of a QCM sensor was designed. Finite element simulation using COMSOL Multiphysics was implemented to detect VOCs involving acetone, and IPA using chitosan sensing layer at 1000 ppm concentration of analyte gas. Greater frequency shift was observed for gases with greater molar mass for both simulation and experimental work. Additionally, the functional groups of chitosan, as well as the functional groups of both acetone and IPA analyte gases, have altered the detection selectivity. In simulation work, chitosan sensing layer shows slightly higher sensitivity towards IPA analyte gas molecules at 0.06232 Hz/ppm than acetone analyte gas at 0.06076 Hz/ppm. This is due to the greater molecular mass of IPA compared to acetone analyte gas. The simulation results have been validated through experimental work where the frequency shift measured for acetone at 41.3 Hz is lower than IPA at 84.8 Hz. Further studies will be implemented to investigate the effect of environmental condition performance of the QCM gas sensor as different volatile organic compounds that behave differently according to their chemical properties.

Acknowledgement

This work was fully supported by the Fundamental Research Grant Scheme (FRGS19-136-0745) (Grant No: FRGS/1/2019/TK04/UIAM/02/3) from Ministry of Higher Education (MOHE).

References

- [1] G. D. Thurston, *Outdoor Air Pollution: Sources, Atmospheric Transport, and Human Health Effects*, Second Edition., vol. 5, no. 69. Elsevier, 2016.
- [2] N. L. Lukman Hekiem et al., "Advanced vapour sensing materials: Existing and latent to acoustic wave sensors for VOCs detection as the potential exhaled breath biomarkers for lung cancer," *Sensors Actuators A. Phys.*, vol. 329, no. 2021, p. 112792, 2021, [Online]. Available: <https://doi.org/10.1016/j.sna.2021.112792>.
- [3] J. Rudnicka, M. Walczak, T. Kowalkowski, T. Jezierski, and B. Buszewski, "Determination of volatile organic compounds as potential markers of lung cancer by gas chromatography-mass spectrometry versus trained dogs," *Sensors Actuators, B Chem.*, vol. 202, pp. 615–621, 2014, doi: 10.1016/j.snb.2014.06.006.
- [4] Y. Saalberg and M. Wolff, "Clinica Chimica Acta VOC breath biomarkers in lung cancer," *Clin. Chim. Acta*, vol. 459, pp. 5–9, 2016, doi: 10.1016/j.cca.2016.05.013.
- [5] R. Capuano, A. Catini, R. Paolesse, and C. Di Natale, "Sensors for Lung Cancer Diagnosis," *J. Clin. Med.*, vol. 8, no. 2, p. 235, 2019, doi: 10.3390/jcm8020235.
- [6] L. Reijnders and M. A. J. Huijbregts, "Palm oil and the emission of carbon-based greenhouse gases," *J. Clean. Prod.*, vol. 16, no. 4, pp. 477–482, 2008, doi: 10.1016/j.jclepro.2006.07.054.
- [7] A. Meijide et al., "Measured greenhouse gas budgets challenge emission savings from palm-oil biodiesel," *Nat. Commun.*, vol. 11, no. 1, pp. 1–11, 2020, doi: 10.1038/s41467-020-14852-6.
- [8] B. L. McVicker, D. J. Tuma, A. A. Naji, and C. A. Casey, *Alcohol and Apoptosis*, vol. 3–3. Elsevier Ltd, 2005.
- [9] C. Liu, B. Wyszynski, R. Yatabe, K. Hayashi, and K. Toko, "Molecularly imprinted sol-gel-based QCM sensor arrays for the detection and recognition of volatile aldehydes," *Sensors (Switzerland)*, vol. 17, no. 2, pp. 1–15, 2017, doi: 10.3390/s17020382.
- [10] C. W. Tang, J. W. Zhen, R. C. Wu, P. Y. Ou, C. C. Wang, and C. Bin Wang, "Study on toluene adsorption and desorption performance on nanostructured manganese dioxide-coated quartz crystal microbalance," *Mater. Lett.*, vol. 273, p. 127942, 2020, doi: 10.1016/j.matlet.2020.127942.

- [11] L. Wang, J. Gao, and J. Xu, "QCM formaldehyde sensing materials: Design and sensing mechanism," *Sensors Actuators, B Chem.*, vol. 293, no. December 2018, pp. 71–82, 2019, doi: 10.1016/j.snb.2019.04.050.
- [12] A. Mirzaei, S. G. Leonardi, and G. Neri, "Detection of hazardous volatile organic compounds (VOCs) by metal oxide nanostructures-based gas sensors: A review," *Ceram. Int.*, vol. 42, no. 14, pp. 15119–15141, 2016, doi: 10.1016/j.ceramint.2016.06.145.
- [13] I. Hafaiedh, W. El Euch, P. Clement, E. Llobet, and A. Abdelghani, "Multi-walled carbon nanotubes for volatile organic compound detection," *Sensors Actuators, B Chem.*, vol. 182, pp. 344–350, 2013, doi: 10.1016/j.snb.2013.03.020.
- [14] U. Stahl et al., "Long-term stability of polymer-coated surface transversewave sensors for the detection of organic solvent vapors," *Sensors (Switzerland)*, vol. 17, no. 11, 2017, doi: 10.3390/s17112529.
- [15] F. B. Ahmad, M. H. Maziaty Akmal, A. Amran, and M. H. Hasni, "Characterization of chitosan from extracted fungal biomass for piezoelectric application," *IOP Conf. Ser. Mater. Sci. Eng.*, vol. 778, no. 1, 2020, doi: 10.1088/1757-899X/778/1/012034.
- [16] M. M. Ayad, N. Salahuddin, and I. M. Minisy, "Detection of some volatile organic compounds with chitosan-coated quartz crystal microbalance," *Des. Monomers Polym.*, vol. 17, no. 8, pp. 795–802, 2014, doi: 10.1080/15685551.2014.918019.
- [17] M. M. Ayad, N. A. Salahuddin, I. M. Minisy, and W. A. Amer, "Chitosan/polyaniline nanofibers coating on the quartz crystal microbalance electrode for gas sensing," *Sensors Actuators, B Chem.*, vol. 202, pp. 144–153, 2014, doi: 10.1016/j.snb.2014.05.046.
- [18] A. American and N. Standard, "An American National Standard: IEEE Standard on Piezoelectricity," *IEEE Trans. Sonics Ultrason.*, vol. 31, no. 2, pp. 8–10, 1984, doi: 10.1109/T-SU.1984.31464.
- [19] Z. Sabani, A. A. M. Ralib, J. Karim, N. B. Saidin, and N. F. B. M. Razali, "Design and simulation of Film Bulk Acoustic Wave Resonator (FBAR) Gas Sensor Based on ZnO Thin Film," *Proc. 2019 IEEE Reg. Symp. Micro Nanoelectron. RSM 2019*, pp. 34–37, 2019, doi: 10.1109/RSM46715.2019.8943566.
- [20] N. L. Lukman Hekiem et al., "Effect of chitosan dissolved in different acetic acid concentration towards VOC sensing performance of quartz crystal microbalance overlay with chitosan," *Mater. Lett.*, vol. 291, p. 129524, 2021, doi: 10.1016/j.matlet.2021.129524.
- [21] A. K. Havare, H. Ilgu, S. Okur, and G. Sanl-Mohamed, "Humidity sensing properties of chitosan by using quartz crystal microbalance method," *Sens. Lett.*, vol. 10, no. 3–4, pp. 906–910, 2012, doi: 10.1166/sl.2012.2585.
- [22] S. Ondaral, E. Çelik, O. Ç. Kurtuluş, E. Aşıkuzun, and İ. Yakın, "Chitosan adsorption on nanofibrillated cellulose with different aldehyde content and interaction with phosphate buffered saline," *Carbohydr. Polym.*, vol. 186, no. October 2017, pp. 192–199, 2018, doi: 10.1016/j.carbpol.2017.12.028.
- [23] M. Kołodziejaska, K. Jankowska, M. Klak, and M. Wszola, "Chitosan as an underrated polymer in modern tissue engineering," *Nanomaterials*, vol. 11, no. 11. 2021, doi: 10.3390/nano11113019.
- [24] N. L. Lukman Hekiem, A. A. Md Ralib, M. A. M. Hatta, F. B. Ahmad, R. A. Rahim, and N. F. Za'bah, "Performance Analysis of VOCs Detection using Polyisobutylene and Chitosan Overlaid on QCM Sensor," in *Proceedings - 2021 IEEE Regional Symposium on Micro and Nanoelectronics, RSM 2021*, 2021, pp. 157–160, doi: 10.1109/RSM52397.2021.9511614.
- [25] D. Tsaneva, Z. Petkova, N. Petkova, M. Stoyanova, A. Stoyanova, and P. Denev, "Isolation and characterization of chitin and biologically active substances from honeybee (*Apis mellifera*)," *J. Pharm. Sci. Res.*, vol. 10, no. 4, pp. 884–888, 2018.
- [26] Z. Q. Lei et al., "Group exchange between ketones and carboxylic acids through directing group assisted Rh-catalyzed reorganization of carbon skeletons," *J. Am. Chem. Soc.*, vol. 137, no. 15, pp. 5012–5020, 2015, doi: 10.1021/ja512003d.
- [27] K. Triyana et al., "Chitosan-Based Quartz Crystal Microbalance for Alcohol Sensing," *Electronics*, vol. 7, no. 9, p. 181, 2018, doi: 10.3390/electronics7090181.
- [28] S. Ni et al., "A Radical Approach to Anionic Chemistry: Synthesis of Ketones, Alcohols, and Amines," *J. Am. Chem. Soc.*, vol. 141, no. 16, pp. 6726–6739, 2019, doi: 10.1021/jacs.9b02238.
- [29] Pevzner, "乳鼠心肌提取 HHS Public Access," *Physiol. Behav.*, vol. 176, no. 3, pp. 139–148, 2017, doi: 10.1016/j.tetlet.2019.151505.Nucleophilic.
- [30] B. Sahariah and B. K. Sarma, "Relative orientation of the carbonyl groups determines the nature of orbital interactions in carbonyl-carbonyl short contacts," *Chem. Sci.*, vol. 10, no. 3, pp. 909–917, 2019, doi: 10.1039/c8sc04221g.
- [31] M. Jelkmann et al., "Chitosan: The One and Only? Aminated Cellulose as an Innovative Option for Primary Amino Groups Containing Polymers," *Biomacromolecules*, vol. 19, no. 10, pp. 4059–4067, 2018, doi: 10.1021/acs.biomac.8b01069.
- [32] X. Wang, B. Ding, M. Sun, J. Yu, and G. Sun, "Nanofibrous polyethyleneimine membranes as sensitive coatings for quartz crystal microbalance-based formaldehyde sensors," *Sensors Actuators, B Chem.*, vol. 144, no. 1, pp. 11–17, 2010, doi: 10.1016/j.snb.2009.08.023.

- [33] T. Yan, B. L. Feringa, and K. Barta, "Iron catalysed direct alkylation of amines with alcohols," *Nat. Commun.*, vol. 5, pp. 1–7, 2014, doi: 10.1038/ncomms6602.
- [34] M. N. Fini, S. Soroush, and M. M. Montazer-Rahmati, "Synthesis and optimization of chitosan ceramic-supported membranes in pervaporation ethanol dehydration," *Membranes (Basel)*, vol. 8, no. 4, 2018, doi: 10.3390/membranes8040119.